FULL PAPER

Dalton
www.rsc.org/dalton

Cation and hydrogen bonding effects on the self-association and luminescence of the dicyanoaurate ion, $[Au(CN)_2]^-$

Matthias Stender,[a] Marilyn M. Olmstead,[a] Alan L. Balch,*[a] Daniel Rios[b] and Saeed Attar*[b]

[a] *Department of Chemistry, University of California Davis, California 95616, USA. E-mail: albalch@ucdavis.edu*

[b] *Department of Chemistry, California State University Fresno, California 93740, USA. E-mail: sattar@csufresno.edu*

Received 21st August 2003, Accepted 9th September 2003
First published as an Advance Article on the web 23rd September 2003

The colorless salts $[C_5H_{10}NH_2][Au^I(CN)_2]$, $[C_4H_8NH_2][Au^I(CN)_2]$, $[Ph_2NNH_3][Au^I(CN)_2]\cdot H_2O$ and $[(n\text{-}C_3H_7)_4N][Au^I(CN)_2]\cdot H_2O$ have been prepared by evaporation of aqueous solutions of potassium dicyanoaurate and the chloride salt of the appropriate cation. Hydrogen bonding between the cations and the cyano groups of the anions facilitates the formation of structures with strong aurophilic interactions between the anions. Thus, the $[Au(CN)_2]^-$ ions self-associate in the three salts $[C_5H_{10}NH_2][Au^I(CN)_2]$ (Au ⋯ Au 3.0969(3) Å), $[C_4H_8NH_2][Au^I(CN)_2]$ (Au1 ⋯ Au2 3.0795(4) Å), $[Ph_2NNH_3][Au^I(CN)_2]\cdot H_2O$ (Au ⋯ Au 3.0866(4) Å), while in $[(n\text{-}C_3H_7)_4N][Au^I(CN)_2]\cdot H_2O$, which lacks N–H units, the gold ions are widely dispersed. The crystals of $[C_5H_{10}NH_2][Au^I(CN)_2]$, $[C_4H_8NH_2][Au^I(CN)_2]$ and $[Ph_2NNH_3][Au^I(CN)_2]\cdot H_2O$ each show strong blue luminescence at room temperature, while $[(n\text{-}C_3H_7)_4N][Au^I(CN)_2]\cdot H_2O$ is non-luminescent.

Introduction

The high chemical stability of the dicyanoaurate ion, $[Au(CN)_2]^-$, contributes to its many uses. Thus dicyanoaurate is involved in the processing of gold ores,[1] in the electroplating of gold,[2] as a precursor to gold–ruby glass,[3] and in protein crystallography as a phasing agent.[4] Dicyanoaurate is a metabolite from gold(I) drugs such as auranofin and allochrysine.[5]

Linear, two-coordinate gold(I) complexes are well known to undergo self-association through aurophilic attractions[6,7] which result from a combination of relativistic and electron correlation effects.[8–10] Generally, aurophilic attractions result in close approach of Au(I) centers with Au ⋯ Au separations of <3.6 Å.[11,12]

There have been a number of crystallographic studies of compounds containing $[Au(CN)_2]^-$. Recently, however, in reviewing the available crystal structures of materials containing $[Au(CN)_2]^-$, Schmidbaur and co-workers noted that anion aggregation occurred only in "very special cases".[13] The majority of the known structures showed the linear $[Au(CN)_2]^-$ unit surrounded by cations. Aggregation of the linear $[Au(CN)_2]^-$ would appear to be disfavored on coulombic grounds, but the simple linear structure itself would seem to encourage self-association through aurophilic interactions.

Several studies by Patterson and co-workers have shown that $[Au(CN)_2]^-$ aggregates under a variety of conditions in both the solid state and in solution.[14–16] The aggregated forms display variations in their luminescence. For example, the luminescence from solutions of $K[Au(CN)_2]$ can be "tuned" so that λ_{max} varies from 275 to 470 nm depending upon the concentration and solvent.[17] The resulting luminescence has been attributed to excited state interactions in oligomeric forms of this anion.[14–17] For a simple dimer, the orbitals involved are an antibonding HOMO with largely d_{z^2} character and a bonding LUMO with largely p_z character, where the z axis connects adjacent gold centers. Because of the unusual combination of a antibonding HOMO and a bonding LUMO, the Au ⋯ Au attraction is stronger in the excited state than in the ground state.

Recent studies of the gold(I) complexes, $[(CyNC)_2Au^I]^+$ and $[Au\{C(NHMe)_2\}_2]^+$, have shown that these cations can undergo significant self-association in the solid state and that this aggregation is dependent on the chemical identity of the anions involved.[18–20] For example $[(CyNC)_2Au^I]^+$ in $[(CyNC)_2Au^I](PF_6)$ self-associates to form two crystalline polymorphs. The colorless polymorph contains a linear chain of cations with a short Au ⋯ Au contact of 3.1822(3) Å, while the yellow polymorph contains four independent cations that are organized into kinked, infinite chains with shorter Au ⋯ Au contacts of 2.9800(5), 2.9784(5), 2.9652(5) and 2.9648(5) Å. Both polymorphs are luminescent with λ_{max} for the colorless form at 424 nm and λ_{max} for the yellow form at 480 nm. However, solutions of either polymorph are colorless and non-luminescent as a result of dissociation of the individual ions in solution. Since these cations readily self-associate, we wondered whether $[Au(CN)_2]^-$ could be encouraged to aggregate by forming salts with primary and secondary amines. Such ammonium ions could form hydrogen bonds with the nitrogen atoms of the anion and stabilize anion self-association through a combination of hydrogen bonding and other coulombic interactions. Here we report that close approach of $[Au(CN)_2]^-$ ions can be achieved in this fashion.

Results

The colorless salts, $[C_5H_{10}NH_2][Au^I(CN)_2]$, $[C_4H_8NH_2][Au^I(CN)_2]$, $[Ph_2NNH_3][Au^I(CN)_2]$ and $[(n\text{-}C_3H_7)_4N][Au^I(CN)_2]$ have been obtained by mixing aqueous solutions of potassium dicyanoaurate with aqueous or methanolic solutions containing the appropriate cation and allowing these solutions to slowly evaporate.

The structure of $[C_5H_{10}NH_2][Au^I(CN)_2]$

The asymmetric unit consists of one anion and one cation in general positions. Selected interatomic distances and angles are given in Table 1 for all of the new compounds reported here. The dimensions of the anion and cation with its chair conformation are normal. As seen in Fig. 1, the anions are arranged into columns with a remarkably short Au ⋯ Au distance of 3.0969(3) Å. The extended chains of anions are slightly bent with an Au ⋯ Au ⋯ Au angle of 165.108(7)°. Adjacent $[Au^I(CN)_2]^-$ ions have a nearly staggered orientation with a C1–Au1 ⋯ Au1B–C1B dihedral angle of 64.8°.

Cations are situated between the chains of anions, and the amino protons are hydrogen bonded to the cyano groups of anions in adjacent chains as seen in Fig. 1. Fig. 2 shows the unit cell and the parallel arrangements of the chains.

DOI: 10.1039/b310085e

Table 1 Selected bond lengths (Å) and bond angles (°) for $[Au^{I}(CN)_2]^-$ salts

	$[C_5H_{10}NH_2]$ $[Au^{I}(CN)_2]$	$[C_4H_8NH_2]$ $[Au^{I}(CN)_2]$	$[Ph_2NNH_3][Au^{I}(CN)_2]\cdot H_2O$	$[n\text{-}Pr_4N]$ $[Au^{I}(CN)_2]\cdot H_2O$
Au1–C1	1.987(3)	1.988(5)	1.986(4)	1.989(4)
Au1–C2	1.994(2)		1.985(4)	
C1–N1	1.147(4)	1.147(6)	1.143(5)	1.139(5)
C2–N2	1.144(4)		1.150(5)	
C–Au–C	179.28(11)	178.1(3)	177.78(16)	180

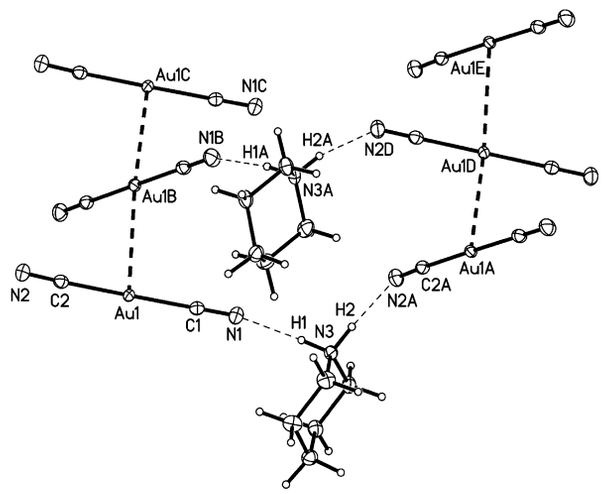

Fig. 1 A view of a portion of the structure of $[C_5H_{10}NH_2][Au^{I}(CN)_2]$ that shows the columns of $[Au^{I}(CN)_2]^-$ ions and the hydrogen bonding interaction between the cations and anions. Selected interatomic distances (Å): Au1 ··· Au1B 3.0969(3), N3H1 ··· N1 1.94, N3 ··· N1 2.849(3), N3H2 ··· N2 1.92, N3 ··· N2 2.824(3). Selected interatomic angles (°): Au1 ··· Au1B ··· Au1C 165.108(7), N3 ··· H1 ··· N1 170.1, N3 ··· H1 ··· N1 167.1.

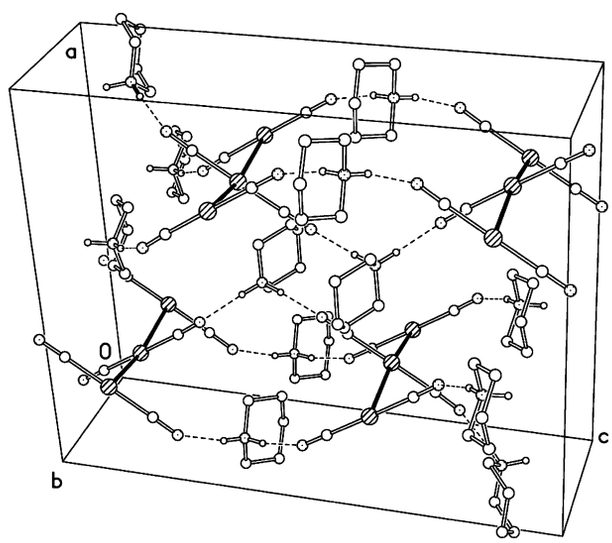

Fig. 2 A view of the unit cell of $[C_5H_{10}NH_2][Au^{I}(CN)_2]$ that shows the interactions between cations and anions. The interactions are shown as bold dashed lines and the hydrogen bonds as thin dashed lines.

The structure of $[C_4H_8NH_2][Au^{I}(CN)_2]$

Selected interatomic distances and angles are given in Table 1. The asymmetric unit consists of two half-anions in special positions and one cation in a general position. Fig. 3 shows a drawing of the chain of anions and the location of one cation which forms a hydrogen bond to an anion. Au1 is situated on a crystallographic center of symmetry while Au2 is located on a crystallographic two-fold axis. The two different anions form a single chain connected by aurophilic interactions with an Au1 ··· Au2 distance of 3.0795(4) Å. Within these chains the Au1 ··· Au2 ··· Au1 portion is linear while the

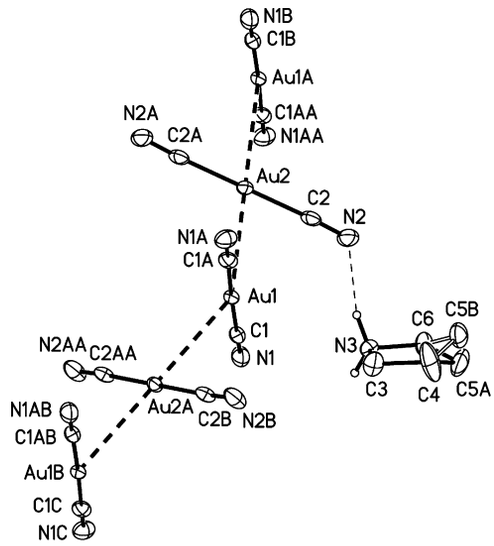

Fig. 3 A view of the structure of $[C_4H_8NH_2][Au^{I}(CN)_2]$ that shows the chains of $[Au^{I}(CN)_2]^-$ ions, the hydrogen bonding interaction between one cation and one anion, and the disorder in the pyrrolidinium ring. Selected interatomic distances (Å): Au1 ··· Au2 3.0795(4), N3 ··· N2 2.851(6). Selected interatomic angles (°): Au2 ··· Au1 ··· Au2A 147.100(9), Au1 ··· Au2 ··· Au1B 180.000(8).

Au2 ··· Au1 ··· Au2 part is bent at an angle of 147.100(9)°. The C1–Au1 ··· Au12–C12 dihedral angle is 54.9° and the neighboring anions are nearly staggered. As seen in Fig. 3, there is disorder that involves one carbon of the pyrrolidinium ring and consequently the ring conformation.

As is the case with $[C_5H_{10}NH_2][Au^{I}(CN)_2]$, the cations are hydrogen-bonded to the nitrogen atoms of the anions. Again each cation spans two adjacent chains. However, the structural motif formed by this interaction is more complex in $[C_4H_8NH_2][Au^{I}(CN)_2]$ than in $[C_5H_{10}NH_2][Au^{I}(CN)_2]$. As seen in the stereoview in Fig. 4, a chain of anions in $[C_4H_8NH_2][Au^{I}(CN)_2]$ is connected to four other similar chains through hydrogen bonding to the cations.

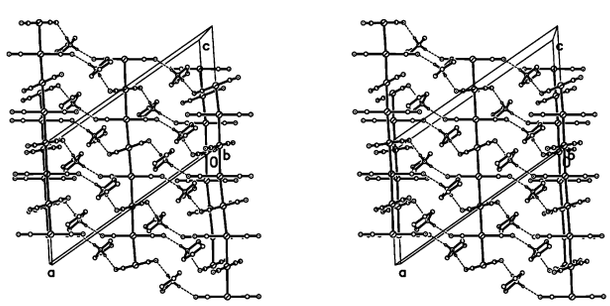

Fig. 4 A stereoview of the structure of $[C_4H_8NH_2][Au^{I}(CN)_2]$ that shows five chains of $[Au^{I}(CN)_2]^-$ ions and the way the cations form hydrogen bond between the chains. In this drawing the Au ··· Au interactions are shown as solid lines.

The structure of $[Ph_2NNH_3][Au^{I}(CN)_2]\cdot H_2O$

There are one cation, one anion, and one water molecule in the asymmetric unit. These components are interconnected through a combination of aurophilic attractions and hydrogen bonds as

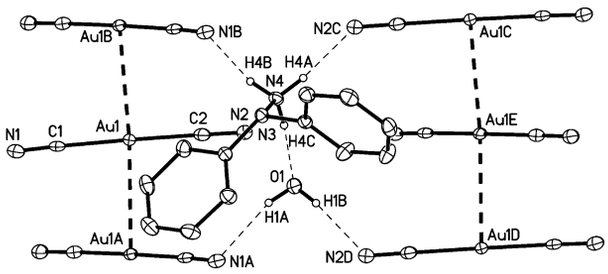

Fig. 5 A view of the structure of $[Ph_2NNH_3][Au^I(CN)_2]\cdot H_2O$ that shows two chains of $[Au^I(CN)_2]^-$ ions and the hydrogen bonding interactions that run parallel to these chain. Selected interatomic distances (Å): Au1 ··· Au1A 3.0866(4), N4H4A ··· N2C 1.96 N4 ··· N2C 2.864(4), N4 ··· N1B 2.859(4), N4 ··· O1 2.788(4), N1A ··· O1 2.913(4), N2D ··· O1 2.925(4). Selected interatomic angle (°): Au1A ··· Au1 ··· Au1B 175.635(9).

seen in Fig. 5. The aurophilic attractions produce a column of anions with a Au ··· Au separation of 3.0866(4) Å. The chain is slightly bent at each gold ion with an Au ··· Au ··· Au angle of 175.635(9)°. Within the column the anions are staggered with a dihedral C1–Au1–Au1′–C1′ angle of 55.3°.

One of the N–H protons of the cation is hydrogen bonded to N1 of the anion, while another is hydrogen bonded to a water molecule. The water molecule in turn is hydrogen bonded to a nitrogen atom of another anion. These interactions produce a pattern of alternating cations and water molecules that runs parallel to the chain of anions and interacts with that chain through hydrogen bonds to the nitrogen atoms of every other anion as seen in Fig. 5. Fig. 6 shows a packing diagram for a larger portion of the solid and reveals how the units shown in Fig. 5 are put together. Each column of anions make hydrogen bonding contacts with four rows of alternating $[Ph_2NNH_3]^+$ ions and water molecules. In this fashion sheets of cations, water molecules and anions are created that run parallel to the crystallographic *ab* plane. These sheets interact with one another through van der Waals interactions between the phenyl rings of the cations. Note that the phenyl rings protrude on either side of the sheets.

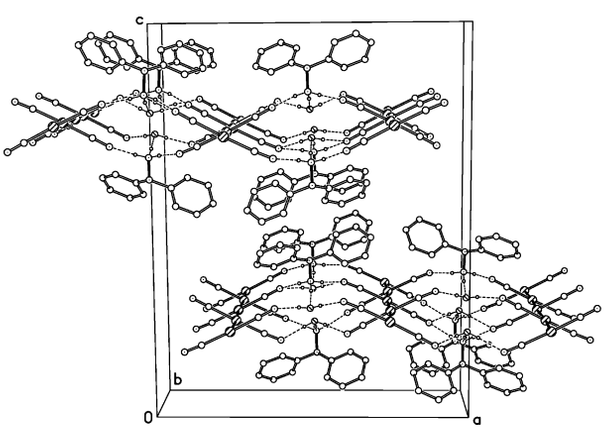

Fig. 6 A view of the unit cell of $[[Ph_2NNH_3][Au^I(CN)_2]\cdot H_2O$ that shows the interactions between cations, anions and water molecules.

The structure of $[(n\text{-}C_3H_7)_4N][Au^I(CN)_2]\cdot H_2O$

The asymmetric unit consists of one half of a cation, one half of an anion and one half of a water molecule. The gold ion is positioned at a center of symmetry while the nitrogen and oxygen atoms are located on two-fold axes. A view of the structure is shown in Fig. 7. A water molecule is hydrogen bonded to the nitrogen atoms of two anions to form an extended zig-zag array of these units. As a consequence, the gold ions are widely separated. The shortest distance between gold ions in this array is 7.526(1) Å. Fig. 8 shows how the components shown in Fig. 7

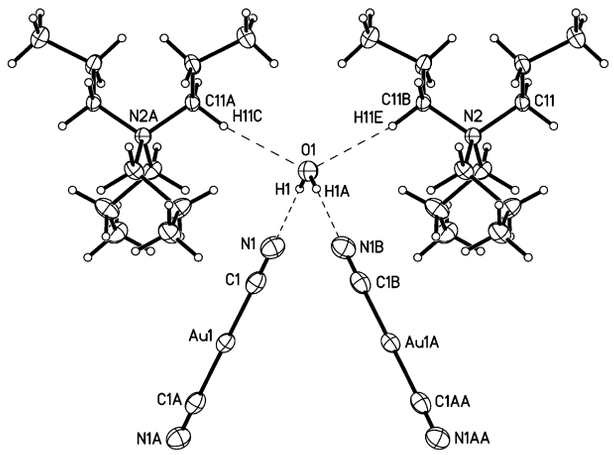

Fig. 7 A view of the structure of $[n\text{-}Pr_4N][Au^I(CN)_2]\cdot H_2O$ that shows the interactions between the $[Au^I(CN)_2]^-$ ions and the water molecules. Selected interatomic distances (Å): Au1 ··· Au1#1 7.526(1), N1 ··· O1 2.920(4).

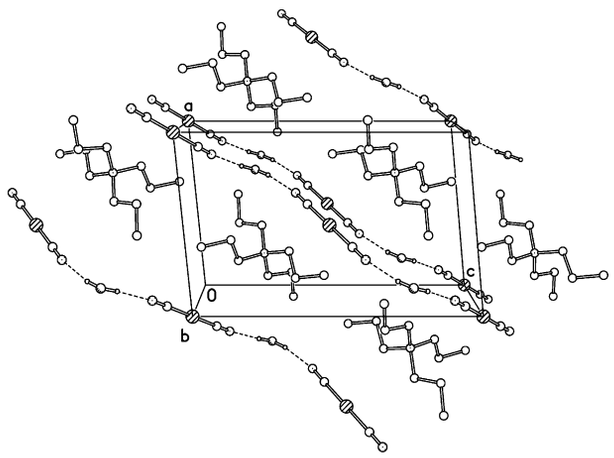

Fig. 8 A drawing of $[n\text{-}Pr_4N][Au^I(CN)_2]\cdot H_2O$ which shows the layering of the anions and their hydrogen bonded water molecules and the cation.

are interleaved in the crystal. The cations lie in spaces between the anions and water molecules which run diagonally along the unit cell. The closest contact between gold ions in different zigzag arrays is 8.1387(12) Å, the length of the crystallographic *b* axis.

Luminescence

Colorless crystals of $[C_5H_{10}NH_2][Au^I(CN)_2]$, $[C_4H_8NH_2][Au^I(CN)_2]$ and $[Ph_2NNH_3][Au^I(CN)_2]\cdot H_2O$ show intense blue photoluminescence at room temperature. The emission and excitation spectra of $[C_5H_{10}NH_2][Au^I(CN)_2]$ at 298 K are shown in Fig. 9. There is a strong, broad emission with a maximum at 436 nm. The excitation profile shows a maximum at 378 nm with a shoulder at 292 nm. The emission spectrum does not change when the excitation wavelength is altered.

As seen in Fig. 10, the luminescence from $[C_4H_8NH_2][Au^I(CN)_2]$ is similar. At 298 K, the emission spectrum consists of a broad, symmetrical band with λ_{max} of 451 nm. The excitation profile shows maxima at 405, 385, 360 and 328 nm, but excitation at each of these wavelengths produces the same emission spectrum as that shown in Fig. 10.

Crystals of $[Ph_2NNH_3][Au^I(CN)_2]\cdot H_2O$ show a broad emission at 400 nm with an excitation maximum at 350 nm.

Crystalline $[(n\text{-}C_3H_7)_4N][Au^I(CN)_2]\cdot H_2O$ with its widely separated gold centers is non-luminescent at room temperature and at 77 K. Likewise, we have observed that $[(n\text{-}C_4H_9)_4N][Au^I(CN)_2]$, which also has widely dispersed anions with long distances between gold ions,[21] is non-luminescent.

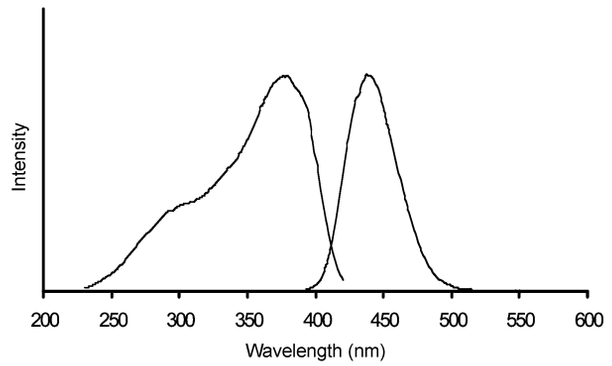

Fig. 9 Emission and excitation spectra of crystalline $[C_5H_{10}NH_2][Au^I(CN)_2]$ at 298 K.

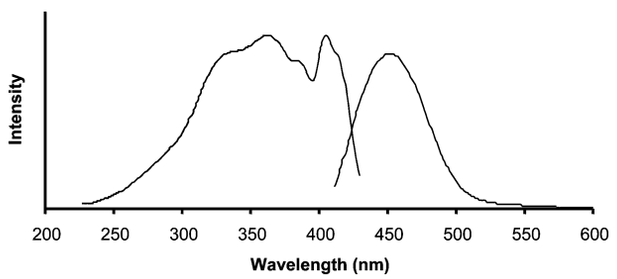

Fig. 10 Emission and excitation spectra of crystalline $[C_4H_8NH_2][Au^I(CN)_2]$ at 298 K.

Discussion

The results reported here show that close contact between $[Au(CN)_2]^-$ ions can be promoted through the use of ammonium ions whose H–N–H units form hydrogen bonds to the anions. These hydrogen bonds insure close proximity of the cations to the anions and help to minimize the coulombic repulsion between the anions. These observations support the conclusions of Schmidbaur and co-workers that additional support in the form of contacts with cations or solvent molecules is needed to promote aurophilic interactions between $[Au(CN)_2]^-$ ions.[13] One other case of a protonated amine facilitating the formation of a chain of $[Au(CN)_2]^-$ ions has been reported.[22] In (2-methylimidazolinium)$[Au(CN)_2]$ a staggered chain of these anions is present with an Au ··· Au distance of 3.25 Å.[22] The chains of $[Au(CN)_2]^-$ ions that are reported here have rather short Au ··· Au contacts that span a narrow range of 3.0795(4)–3.0969(3) Å. For comparison, in $[Pt(NH_3)_4][Au(CN)_2]\cdot 1.5(H_2O)$, which contains a chains of Au–Pt–Au units that intersect *via* Au ··· Au contacts, there are three such contacts between $[Au(CN)_2]^-$ ions with distances of 3.3307(5), 3.2902(5) and 3.1903(4) Å.[23] All of these distances are longer than those seen in the ammonium salts reported here. In related work, Leznoff and co-workers have shown that chains of $[Au(CN)_2]^-$ ions can also be formed by reacting this anion with cationic transition metal complexes.[24–27] Polypyridinium cations have been found to produce crystalline materials that contain $[Au(CN)_2]^-$ ions which aggregate to form trimers, tetramers, or chains.[28]

The Au ··· Au distances in the chains of $[Au(CN)_2]^-$ anions are shorter than the comparable distances between cations in the white polymorph of $[(CyNC)_2Au^I](PF_6)$ (3.1822(3) Å) but longer than those in its yellow polymorph (2.9800(5), 2.9784(5), 2.9652(5), 2.9648(5) Å).[18] Similarly the Au ··· Au distances between cations in $[Au\{C(NHMe)_2\}_2](PF_6)\cdot 0.5Me_2CO$, (3.1882(1) Å) and in $[Au\{C(NHMe)_2\}_2](BF_4)$ (3.4615(2) Å)[19] are longer than those Au ··· Au distances seen in the ammonium salts reported here.

It is also informative to compare the Au ··· Au distances in the above mentioned chains of anions and cation to those in the series of neutral molecules $(RNC)Au^ICN$. The Au ··· Au interactions between these linear molecules create supramolecular structures that fall into three classes with increasing numbers of contacts between gold centers: simple chains, side-by-side chains, and nets.[29] Those with the simple chains structures are the most relevant for our comparisons. Thus, the structures of $(CyNC)Au^ICN$ and $(t\text{-BuNC})Au^ICN$ consist of corrugated chains of the individual molecules which pack about centers of symmetry so that their dipoles are aligned head-to-tail as shown as **A** in Scheme 1.[25,30] In $(CyNC)Au^ICN$ there are two alternating Au ··· Au distances of 3.426(3) and 3.442(3) Å, while in $(t\text{-BuNC})Au^ICN$ there is only one Au ··· Au distance, 3.568 Å.[26] These distances are considerably longer than those seen for the chains of cations and anions discussed above and appear to indicate that dipolar forces weaken the aurophilic attractions in $(RNC)Au^ICN$. With pairs of these rod-like molecules the dihedral angles between the two can vary from the fully eclipsed, shown as **B** in Scheme 1, to the fully staggered shown as **C** . The staggered orientation **C** is the one usually found for the shortest Au ··· Au separations and favors aurophilic attractions, while the eclipsed orientation **B** places the dipoles of the adjacent molecules in proper juxtaposition. For the symmetrical cationic and anionic gold complexes discussed above, these is no dipole contribution to consider, and thus a staggered orientation **C** is present and results in the shorter Au ··· Au separations. For $(RNC)Au^ICN$ the dipolar interaction produces the eclipsed orientation **B** and the Au ··· Au distances are longer. Similarly in the series of neutral, polar molecules, $(RNC)Au^IX$ with X = Cl, Br or I, dipolar factors dominate the situation to the extent that the Au ··· Au separations are weak to non-existent [31] Complexes of the type $(RNC)Au^IX$ form isostructural crystals in which corrugated chains of type A are present. Within these chains the Au ··· Au separations alternate so that with X = Cl the distances are 3.3894(7) and 3.5816(7) Å, but with X = I they increase to 3.7182(11) and 3.9304(12) Å, distances which are well outside the range where aurophilic attractions are significant.[30] Theoretical calculations on $RNC)Au^IX$ indicate that the aurophilic attraction between such molecules is weak.[32]

The luminescent properties of gold(I) complexes has attracted a considerable amount of attention.[33,34] The luminescence observed for crystalline samples of $[C_5H_{10}NH_2][Au^I(CN)_2]$ and $[C_4H_8NH_2][Au^I(CN)_2]$ can be attributed to the presence of aurophilic attractions which have produced the chains of staggered anions in these solids. In contrast, crystals of $[(n\text{-}C_3H_7)_4N][Au^I(CN)_2]\cdot H_2O$ and $[(n\text{-}C_4H_9)_4N][Au^I(CN)_2]$, which have widely separated gold centers, are non-luminescent under similar conditions. These observations are entirely consistent with the studies of Patterson and co-workers who have

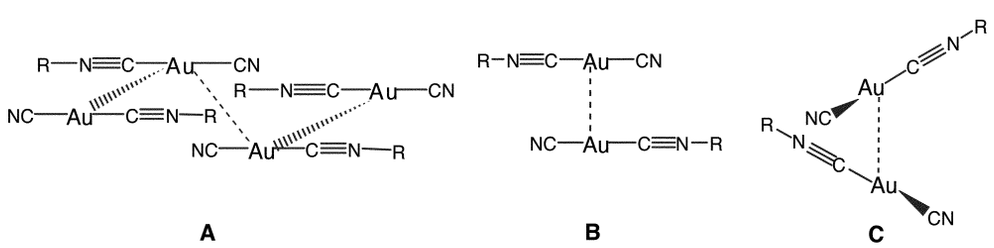

Scheme 1

Table 2 Crystal data and data collection parameters for $[Au^{I}(CN)_2]^-$ salts

	$[C_5H_{10}NH_2][Au^{I}(CN)_2]$	$[C_4H_8NH_2][Au^{I}(CN)_2]$	$[Ph_2NNH_3][Au^{I}(CN)_2]\cdot H_2O$	$[n\text{-}Pr_4N][Au^{I}(CN)_2]\cdot H_2O$
Formula	$C_7H_{12}AuN_3$	$C_6H_{10}AuN_3$	$C_{14}H_{15}AuN_4O$	$C_{14}H_{30}AuN_3O$
M_r	335.16	321.14	452.27	453.38
Color and habit	Colorless block	Colorless needle	Colorless needle	Colorless block
Crystal system	Orthorhombic	Monoclinic	Orthorhombic	Monoclinic
Space group	*Pbca*	*C*2/*c*	*Pbca*	*P*2/*n*
a/Å	15.8490(17)	20.215(3)	19.765(2)	8.3442(12)
b/Å	6.1415(7)	8.5264(11)	6.1688(8)	8.1387(12)
c/Å	19.742(2)	11.8138(15)	24.757(3)	13.351(2)
α/°	90	90	90	90
β/°	90	121.927(2)	90	95.497(2)
γ/°	90	90	90	90
V/Å^3	1921.6(4)	1728.2(4)	3018.5(6)	902.5(2)
T/K	90(2)	190(2)	90(2)	130(2)
Z	8	8	8	2
D_c/g cm^{-3}	2.317	2.468	1.990	1.668
λ(Mo-Kα)/Å	0.71073	0.71073	0.71073	0.71073
μ/mm^{-1}	15.257	16.958	9.748	8.148
Range of transm. factors	0.17–42	0.26–0.63	0.19–0.64	0.44–59
No. unique data	3021	2690	4588	2799
No. parameters refined	101	110	179	92
R^a	0.017	0.024	0.024	0.022
$wR2^b$	0.037	0.053	0.053	0.051

^{a} $R1 = \Sigma||F_o| - |F_c||/\Sigma|F_o|$ (obs. data, $I > 2\sigma(I)$). ^{b} $wR2 = [\Sigma[w(F_o^2 - F_c^2)^2]/\Sigma[w(F_o^2)^2]]^{1/2}$ (all data).

attributed the remarkable variations in the luminescence resulting from $[Au^{I}(CN)_2]^-$ in different environments to the formation of various aggregates.[14–17] The similarities between the emission spectra of $[C_5H_{10}NH_2][Au^{I}(CN)_2]$ and $[C_4H_8NH_2][Au^{I}(CN)_2]$ (Figs. 9 and 10, respectively) reflect the fact that both have nearly staggered chain structures with rather similar Au ··· Au separations.

Experimental

Samples of pyrrolidinium hydrochloride and piperidinium hydrochloride were obtained by adding stoichiometric amounts of the appropriate amine to an aqueous solution of hydrochloric acid. The solution was allowed to evaporate over a week period, after which the colorless crystalline product was collected.

Preparation of $[C_5H_{10}NH_2][Au^{I}(CN)_2]$

A solution of 50 mg (0.17 mmol) of potassium dicyanoaurate in 2 mL of water was added dropwise to a solution of 18.6 mg (0.17 mmol) pyrrolidinium hydrochloride in 2 mL of water. The yellow reaction mixture was filtered and after 3 days of slow evaporation of the solvent, colorless crystals of the product that were suitable for X-ray analysis were formed and removed from the mother-liquor. The yield was 40.1 mg (72%). The product is soluble in water and methanol and slightly soluble in acetonitrile. On heating to 250 °C this salt slowly turns brown but does not melt. IR spectrum: 3448br, 2968s, 2813m, 2553m, 2458w, 2148vs (*ν*(CN)), 1627m, 1464w cm^{-1}.

Preparation of $[C_4H_8NH_2][Au^{I}(CN)_2]$

A solution of 50 mg (0.17 mmol) of potassium dicyanoaurate in 2 mL of water was added dropwise to a solution of 21.0 mg (0.17 mmol) of piperidinium hydrochloride in 2 mL of water. The yellow reaction mixture was filtered. After 4 days of slow evaporation of the solvent, crystals of the product that were suitable for X-ray crystallography were formed. The mother-liquor was removed to produce colorless crystals: 38.2 mg (65%). The product has good solubility in water and methanol. This compound does not melt below 250 °C but does darken during heating. IR spectrum: 3437br, 3008s, 2767m, 2143vs (*ν*(CN)), 1639w, 1402m cm^{-1}.

Preparation of $[Ph_2NNH_3][Au^{I}(CN)_2]\cdot H_2O$

A solution of 53.1 mg (0.18 mmol) of potassium dicyanoaurate in 2 mL of water was added under stirring to a solution of 40.3 mg (0.18 mmol) diphenylhydrazinium hydrochloride in 2 mL of methanol. The reaction mixture was filtered and after slow evaporation of the solvent, crystals suitable for X-ray analysis were formed after 24 h. After removing the mother-liquor with a pipette, the crystals were washed with cold diethyl ether and dried in air. The yield was 57.7 mg (0.13 mmol; 72%). The product is slightly soluble in water and methanol. IR spectrum: *ν*(CN) 2149, 2138 cm^{-1}.

Preparation of $[n\text{-}Pr_4N][Au^{I}(CN)_2]\cdot H_2O$

A solution of 70.8 mg (0.24 mmol) of potassium dicyanoaurate in 2 mL of water was added under stirring to a solution of 66.5 mg (0.25 mmol) tetra(*n*-propyl)ammonium bromide in 2 mL of water and 1 mL of methanol. The reaction mixture was filtered. After slow evaporation of the solvent, crystals suitable for X-ray analysis formed in 3 days. After removal of the mother liquor with a pipette, the crystals were washed with ethanol and diethyl ether and dried in air. The yield was 63.4 mg (0.14 mmol; 60%). The product is soluble in acetonitrile.

Physical measurements

IR spectra were recorded as pressed KBr pellets on a Matteson Galaxie Series FTIR 3000 spectrometer. Electronic absorption spectra were recorded using a Hewlett-Packard 8450A diode array spectrophotometer. Conventional fluorescence excitation and emission spectra were recorded on a Perkin Elmer LS50B luminescence spectrophotometer.

X-Ray crystallography and data collection

The crystals were removed from the glass tubes in which they were grown together with a small amount of mother-liquor and immediately coated with a hydrocarbon oil on the microscope slide. Suitable crystals were mounted on glass fibers with silicone grease and placed in the cold dinitrogen stream of a Bruker SMART CCD with graphite-monochromated Mo-Kα radiation at 90(2) K. No decay was observed in 50 duplicate frames at the end of each data collection. Crystal data are given in Table 2.

The structures were solved by direct methods and refined using all data (based on F^2) using the software of SHELXTL 5.1. A semiempirical method utilizing equivalents was employed to correct for absorption.[35] Hydrogen atoms were added geometrically and refined with a riding model.

CCDC reference numbers 218034–218037.

See http://www.rsc.org/suppdata/dt/b3/b310085e/ for crystallographic data in CIF or other electronic format.

Acknowledgements

We thank the Petroleum Research Fund (Grant 37056-AC) for support. The Bruker SMART 1000 diffractometer was funded in part by NSF Instrumentation grant CHE-9808259.

References

1 M. D. Adams, M. W. Johns and D. W. Dew, in *Gold; Progress in Chemistry, Biochemistry and Technology*, ed. H. Schmidbaur, John Wiley and Sons, New York, 1999, p. 65.
2 R. J. Puddephatt, in *Gold; Progress in Chemistry, Biochemistry and Technology*, ed. H. Schmidbaur, John Wiley and Sons, New York, 1999, p. 235.
3 F. E. Wagner, S. Haslbeck, L. Stievano, S. Calogero, Q. A. Pankhurst and K.-P. Martlinek, *Nature (London)*, 2000, **407**, 691.
4 T. J. Boggon and L. Shapiro, *Structure*, 2000, **8**, R143.
5 F. S. Shaw, III, *Chem. Rev.*, 1999, **99**, 2589.
6 H. Schmidbaur, *Chem. Soc. Rev.*, 1995, **24**, 391.
7 H. Schmidbaur, *Interdisiplinary Sci. Rev.*, 1992, **17**, 213.
8 P. Pyykkö, *Chem. Rev*, 1997, **97**, 597.
9 P. Pyykkö, N. Runeberg and F. Mendizabal, *Chem. Euro. J.*, 1997, **3**, 1451.
10 P. Pyykkö and F. Mendizabal, *Chem. Eur. J.*, 1997, **3**, 1458.
11 P. G. Jones, *Gold Bull.*, 1986, **19**, 46; P. G. Jones, *Gold Bull.*, 1983, **16**, 114; P. G. Jones, *Gold Bull.*, 1981, **14**, 159; P. G. Jones, *Gold Bull.*, 1981, **14**, 102.
12 S. S. Pathaneni and G. R. Desiraju, *J. Chem. Soc., Dalton Trans.*, 1993, 319.
13 R.-Y. Liau, H. Ehlich, A. Schier and H. Schmidbaur, *Z. Naturforsch., Teil B*, 2002, **57**, 1085.
14 M. A. Rawashdeh-Omary, M. A. Omary and H. H. Patterson, *J. Am. Chem. Soc.*, 2000, **122**, 10371.
15 M. A. Rawashdeh-Omary, M. A. Omary, G. E. Shankle and H. H. Patterson, *J. Phys. Chem. B*, 2000, **104**, 6143.
16 M. A. Omary and H. H. Patterson, *J. Am. Chem. Soc.*, 1998, **120**, 7696.
17 M. A. Rawashdeh-Omary, M. A. Omary, H. H. Patterson and J. P. Fackler, Jr., *J. Am. Chem. Soc.*, 2001, **123**, 11237.
18 R. L. White-Morris, M. M. Olmstead and A. L. Balch, *J. Am. Chem. Soc.*, 2003, **125**, 1003.
19 R. L. White-Morris, M. M. Olmstead, F. Jiang, D. S. Tinti and A. L. Balch, *J. Am. Chem. Soc.*, 2002, **124**, 2327.
20 R. L. White-Morris, M. M. Olmstead, F. Jiang and A. L. Balch, *Inorg. Chem.*, 2002, **41**, 2313.
21 R. J. Schubert and K.-J. Range, *Z. Naturforsch., Teil B.*, 1990, 1118.
22 A. H. Schwellnus, L. Denner and J. C. A. Boeyens, *Polyhedron*, 1990, **9**, 975.
23 M. Stender, R. L. White-Morris, M. M. Olmstead and A. L. Balch, *Inorg. Chem.*, 2003, **42**, 4504.
24 C. J. Shorrock, B.-Y. Xue, P. B. Kim, R. J. Batchelor, B. O. Patrick and D. B. Leznoff, *Inorg. Chem.*, 2002, **41**, 6743.
25 D. B. Leznoff, B.-Y. Xue, R. J. Batchelor, F. W. B. Einstein and B. O. Patrick, *Inorg. Chem.*, 2001, **40**, 6026.
26 D. B. Leznoff, B.-Y. Xue, B. O. Patrick, V. Sanchez and R. C. Thompson, *Chem. Commun.*, 2001, 259.
27 D. B. Leznoff, B.-Y. Xue, C. L. Stevens, A. Storr, R. C. Thompson and B. O. Patrick, *Polyhedron*, 2001, **20**, 1247.
28 R. E. Cramer, D. W. Smith and W. VanDoorne, *Inorg. Chem*, 1998, **37**, 5895.
29 R. L. White-Morris, M. Stender, D. S. Tinti, A. L. Balch, D. Rios and S. Attar, *Inorg. Chem*, 2003, **42**, 3237.
30 C.-M. Che, H.-K. Yip, W.-T. Wong and T.-F. Lai, *Inorg. Chim. Acta*, 1992, **197**, 177.
31 R. L. White-Morris, M. M. Olmstead, A. L. Balch, O. Elbjeirami and M. A. Omary, *Inorg. Chem.*, in press.
32 R.-Y. Liau, T. Mathieson, A. Schier, R. J. Berger, N. Runeberg and H. Schmidbaur, *Z. Naturforsch., Teil B*, 2002, **57**, 881.
33 J. M. Forward, J. P. Fackler, Jr. and Z. Assefa, in *Optoelectronic Properties of Inorganic Compounds*, ed. D. M. Roundhill and J. P. Fackler, Jr, Plenum Press, New York, 1999, p. 195.
34 V. W. W. Yam and K. K. W. Lo, *Chem. Soc. Rev.*, 1999, **28**, 323.
35 SADABS 2.0: G. M. Sheldrick, based on a method of R. H. Blessing, *Acta Crystallogr., Sect. A*, 1995, **51**, 33.